Digital pulse shape discrimination methods for n-γ separation in an EJ-301 liquid scintillation detector *

WAN Bo(万波)[1,2] ZHANG Xue-Ying(张雪荧)[1;1)] CHEN Liang(陈亮)[1] GE Hong-Lin(葛红林)[1]
MA Fei(马飞)[1] ZHANG Hong-Bin(张宏斌)[1] JU Yong-Qin(鞠永芹)[1]
ZHANG Yan-Bin(张艳斌)[1] LI Yan-Yan(李严严)[1,2] XU Xiao-Wei(许晓伟)[1,2]

[1] Institute of Modern Physics, Chinese Academy of Sciences, Lanzhou 730000, China
[2] University of Chinese Academy of Sciences, Beijing 100049, China

Abstract: A digital pulse shape discrimination system based on a programmable module NI-5772 has been established and tested with an EJ-301 liquid scintillation detector. The module was operated by running programs developed in LabVIEW, with a sampling frequency up to 1.6 GS/s. Standard gamma sources ^{22}Na, ^{137}Cs and ^{60}Co were used to calibrate the EJ-301 liquid scintillation detector, and the gamma response function was obtained. Digital algorithms for the charge comparison method and zero-crossing method have been developed. The experimental results show that both digital signal processing (DSP) algorithms can discriminate neutrons from γ-rays. Moreover, the zero-crossing method shows better n-γ discrimination at 80 keVee and lower, whereas the charge comparison method gives better results at higher thresholds. In addition, the figure-of-merit (FOM) for detectors of two different dimensions were extracted at 9 energy thresholds, and it was found that the smaller detector presented better n-γ separation for fission neutrons.

Key words: EJ-301 liquid scintillation detector, digital signal processing, charge comparison method, zero-crossing method

PACS: 29.30.Hs, 29.40.Mc, 29.85.Ca **DOI:** 10.1088/1674-1137/39/11/116201

1 Introduction

For the last few decades, the concepts of accelerator-driven subcritical systems (ADS) and spallation neutron sources (SNS) have been proposed and constructed based on spallation reactions [1–3]. High intensity neutron flux and γ-rays are produced around the spallation targets in such systems. Various kinds of neutron detectors, including fission chambers, ^{3}He counters and organic liquid scintillation detectors, have been used to monitor the leakage neutrons in real time in mixed neutron-γ ray radiation environments. Of these detectors, EJ-301 liquid scintillation detectors have been widely employed because of their excellent neutron-γ discrimination, high efficiency for fast neutron detection and superior time resolution. Aiming to discriminate neutrons from γ-rays for the EJ-301 liquid scintillation detector, two common pulse shape discrimination (PSD) methods can be used. One of these is the zero-crossing method, which extracts the zero-crossing time of suitably shaped bipolar pulses [4, 5]. The other is the charge comparison method, based on independent measurements of the integrated charge over two different time regions of the pulse [6, 7].

Recently, with the development of field programmable gate array (FPGA) technology and computer CPUs, digital signal processing (DSP) is now possible. The major difference between analog and DSP techniques is that with the digital method, the current pulse from the anode of photomultiplier tube (PMT) is digitized immediately and all operations are carried out in a software package. For the analog PSD methods, the operations have to be implemented based on CAMAC or VME modules along with a series of complicated analog circuits. The DSP system offers significant advantages over the analog systems in convenience, real-time processing and reduced space requirements by the elimination of extra electronic modules. Prior to this work, some research groups have investigated the DSP method, and performed comparisons of the n-γ separation results using the zero-crossing method and charge comparison method, respectively [8, 9]. However, their experimental

Received 6 February 2015
∗ Supported by National Natural Science Foundation of China (91226107, 11305229) and the Strategic Priority Research Program of the Chinese Academy of Sciences (XDA03030300)
1) E-mail: zhxy@impcas.ac.cn

results showed different behaviours in the ability of n-γ discrimination. For example, when comparing the zero-crossing method and charge comparison method, the results in Ref. [8] suggested the former showed better n-γ separation properties, whereas the conclusion in Ref. [9] was the reverse. Therefore, it is essential to further develop the DSP method and reinvestigate the zero-crossing method and charge comparison method.

In this paper, a digital acquisition system based on the NI-5772 adapter module has been developed. The algorithms for the digital pulse shape discrimination method for n-γ separation in the EJ-301 liquid scintillation detector are described in Section 2. The liquid scintillation detector was calibrated by standard γ-rays sources, and the capacity for n-γ discrimination of the new system was tested with a ^{252}Cf neutron source. At the same time, the capacity for n-γ discrimination of two different dimensions of liquid scintillation detector was also studied.

2 Experimental details

2.1 Algorithm for PSD

Fig. 1(a) presents the typical current pulses related to neutrons and γ-rays. A pulse generated by a γ-ray decays faster to the baseline than a neutron-induced pulse. The major difference between these two pulses occurs in their tail. This is what allows neutrons and γ-rays to be discriminated by analyzing the contributions of slow components to the total light output.

In this paper, two types of digital data processing techniques are employed for n-γ discrimination. One of these is the digital implementation of the conventional charge comparison method. $Q_{\rm total}$ and $Q_{\rm slow}$ represent the total charge of the current pulse and the charge in the slow components, respectively, as shown in Fig. 1(a). Thus neutrons and γ-rays could be separated accurately in mixed radiation fields through comparing the difference of $Q_{\rm slow}$ for each pulse.

The other algorithm is the zero-crossing method. The PMT current signal recorded by a digital oscilloscope is processed via a virtual differentiator-integrator-integrator ($C_1R_1-(R_2C_2)^2$) shaping network, and is finally converted to a bipolar pulse, as shown in Fig. 1(c). The pulse shaping network is performed using a special program written in C++. The difference in the tails of different PMT signals is reflected in the zero-crossing time of the bipolar pulses. To exploit the difference in the zero-crossing time as a parameter for n-γ discrimination, a digital algorithm acting as a constant fraction discriminator (CFD) is used to determine the zero-crossing points. This digital CFD works by finding the shaped signal's maximum and then setting a threshold based on a specific fraction of this maximum.

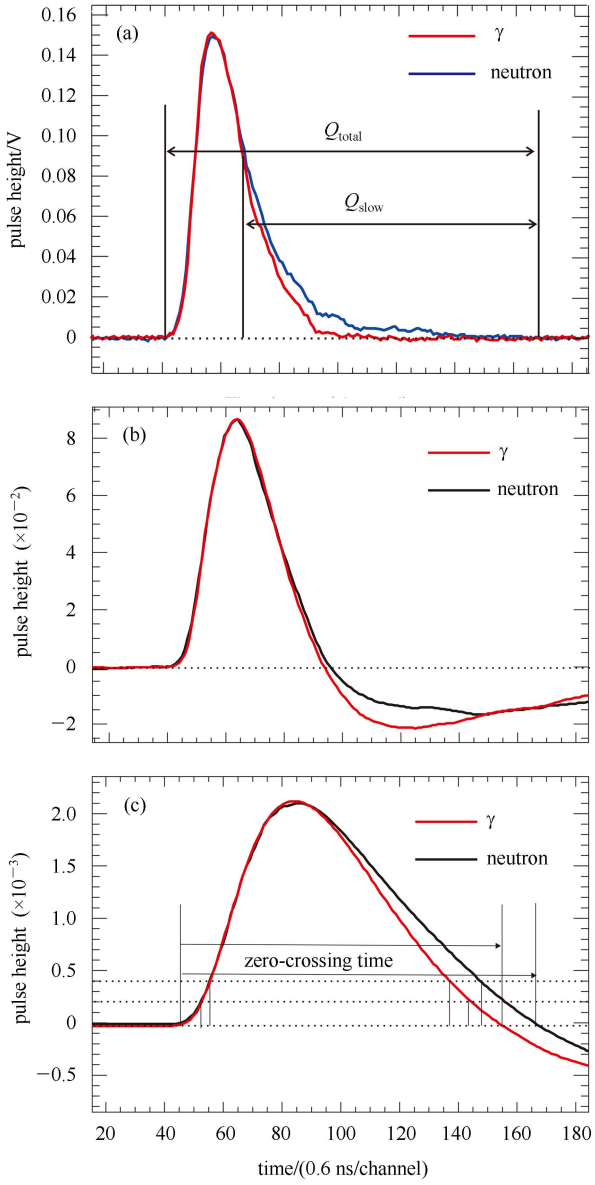

Fig. 1. (color online) (a) Typical PMT signals induced by neutrons and γ-rays. The γ-ray pulse decays more quickly than the neutron pulse, so a small difference can be seen in the tail. (b) PMT signals after the differentiator-integrator ($C_1R_1-R_2C_2$) shaping network. (c) PMT signals after the pulse shaping process ($(C_1R_1-(R_2C_2)^2)$). The γ-ray and neutron pulses cross the zero line at different times.

2.2 Experimental setup

A diagram of experimental setup and electronics is shown in Fig. 2. A cylindrical EJ-301 liquid scintillation detector of diameter 2 inches and length 2 inches, coupled to an ET 9813KB PMT, was used to perform the measurements. The detector was operated with a

negative voltage of 1700 V. The current pulses from anode of the PMT were transferred to an attenuator and then directly digitized using a digital oscilloscope (NI-5772), which could digitize the waveform by running the dedicated LabVIEW data acquisition package. Since this acquisition system could only digitize signals whose maximum voltage range was between -1 V and 1 V, the 9 dB attenuator was employed. In the present work, the digital oscilloscope worked in self-triggering mode with a sampling rate of 1.6 GS/s and 12 bit resolution. A ^{252}Cf neutron source with an intensity of 1.0×10^4 n/s was used to test the n-γ discrimination capability of this system, and standard γ sources were also used for energy calibration of the EJ-301 liquid scintillation detector. Off-line data analysis was performed by running ROOT script files written in C++. In addition, to compare the capability for n-γ discrimination of scintillators with different volumes, another larger liquid scintillation detector of diameter 2 inches and length 4 inches was also employed.

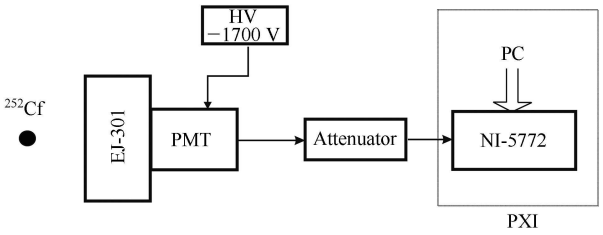

Fig. 2. Experimental setup.

2.3 Energy calibration

In order to determine the effective neutron detection thresholds, the γ energy calibration for the EJ-301 liquid scintillation detector was done with standard γ sources ^{22}Na, ^{137}Cs and ^{60}Co. The positions of the maxima of Compton scattering electrons [10] could be accurately determined through comparing the measured light output spectra with those simulated using GRESP7 code. More details of this method have been described in Refs. [11–13]. The results of calibration together with the light output of ^{22}Na, ^{137}Cs and ^{60}Co are shown in Fig. 3, in which the experimental data is fitted by a linear polynomial.

The γ response function of EJ-301 liquid scintillation detector is expressed by:

$$L=4.94E_{\rm e}-0.095, \quad (1)$$

where L is the light output,and $E_{\rm e}$ is the deposited electron energy for the liquid scintillator in MeV. This calibration is implemented to calculate the equivalent electron energy (MeVee), where 1 MeVee corresponds to the total light output induced by a 1 MeV electron.

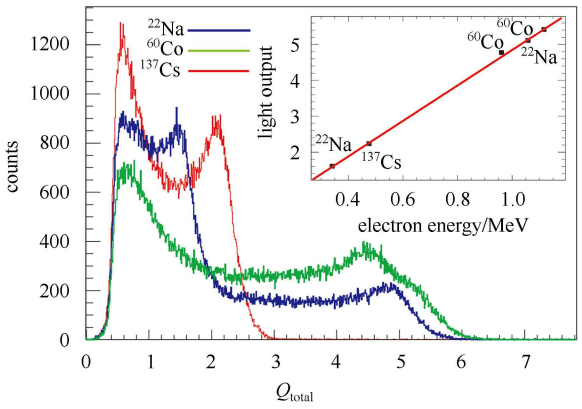

Fig. 3. (color online) Experimental light output for ^{22}Na, ^{137}Cs and ^{60}Co γ sources. The inset shows the calibration result using the Compton edges from the detected spectrum.

3 Results and discussion

3.1 Charge comparison method

A two-dimensional scatter plot of the n-γ discrimination using the charge comparison method at an energy threshold of 180 keVee is shown in Fig. 4. There are two separated strips in the 2D graph, with the upper strip associated with neutrons because of the larger $Q_{\rm slow}$ for equal light output. The overlap is due to the cases of very low energy neutrons and γ-rays, and is the region that determines how well the neutrons are discriminated from γ-rays.

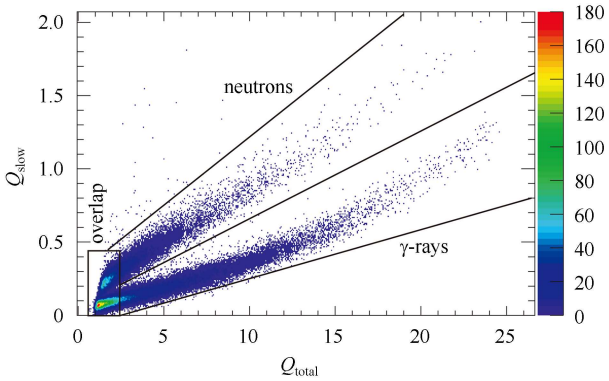

Fig. 4. (color online) 2D plot of $Q_{\rm total}$ versus $Q_{\rm slow}$ for ^{252}Cf source. The energy threshold is 180 keVee.

The quality of n-γ discrimination depends on several factors, such as the algorithms employed, the sampling rate, the type of detector and so on. In order to check the n-γ separation characteristics, a figure-of-merit (FOM) is introduced:

$$\mathrm{FOM}=\frac{\Delta}{\Delta\gamma+\Delta\mathrm{n}}, \quad (2)$$

where Δ is the separation between the peaks of the neutron and γ events. $\Delta\gamma$ and Δn are the FWHM (full width at half maximum) of the γ and neutron peaks, respectively.

FOMs over different time intervals were extracted for the purpose of evaluating the optimum integration intervals for $Q_{\rm slow}$ and $Q_{\rm total}$. The integration intervals were optimized to minimize the number of misclassified pulses. In this work, the total integration was calculated from the beginning of the pulse to 50 ns after the pulse maximum for all the signals. FOMs for different time intervals of $Q_{\rm slow}$ are shown in Fig. 5 at 5 energy thresholds (60 keVee, 120 keVee, 180 keVee, 240 keVee and 300 keVee). It is found that the optimum n-γ separation can be derived when the tail integration starts 21 ns and ends 50 ns after the pulse maximum for all of the studied energy thresholds. The extracted optimum integration intervals will be used for the charge comparison algorithm in the following sections.

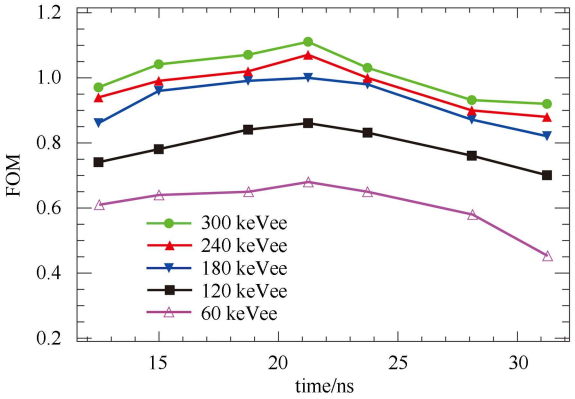

Fig. 5. (color online) FOMs for different integration intervals of $Q_{\rm slow}$; the energy thresholds are 60 keVee, 120 keVee, 180 keVee, 240 keVee and 300 keVee.

3.2 Zero-crossing method

The zero-crossing points were extracted at the position of 0, 0.1 and 0.2 of the bipolar pulses' maximum, as shown in Fig. 1(c), and the FOMs at these situations were 1.27, 1.24 and 1.24, respectively. It is obvious that the zero-crossing method shows optimal n-γ separation properties while the bipolar pulses cross the zero line. A series of FOMs were calculated at different constants for C_1R_1 and R_2C_2, as shown in Table 1. It was found that the optimum n-γ discrimination was achieved when the differentiation time constant (C_1R_1) was 5 ns and the integration time constant (R_2C_2) was 30 ns. Fig. 6 shows the zero-crossing time distribution versus $Q_{\rm total}$ for the same experimental data set. The upper peak corresponds to neutrons because the neutron pulse crosses the baseline much later than the γ pulse. The FOM in this case is 0.91. In order to investigate the effect of energy threshold on the quality of n-γ separation, FOMs at 11 different energy thresholds have been calculated and are shown in Fig. 7. The FOMs are improved from 0.78 to 1.04 when the thresholds increase from 30 keVee to 600 keVee. This phenomenon could be explained by the influence of electronic noise decreasing with larger energy thresholds.

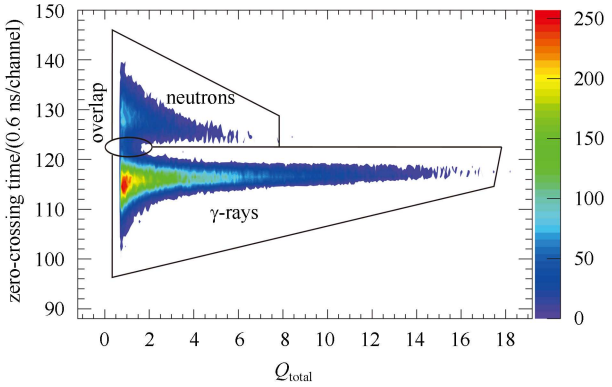

Fig. 6. (color online) 2D plot of zero-crossing time versus $Q_{\rm total}$ for ^{252}Cf source. The energy threshold is 180 keVee.

FOMs calculated using the charge comparison algorithm for the same energy thresholds are also shown in Fig. 7 so as to compare the n-γ separation capacity of the charge comparison and zero-crossing techniques. The contrasting results show that the zero-crossing method is better for energy thresholds of 80 keVee and lower, while for thresholds higher than 80 keVee, the charge comparison method shows optimal n-γ separation properties. Therefore, the zero-crossing method is suitable for outputs lower than 80 keVee and the charge comparison method is the best choice for higher equivalent electron energies. The results are similar to Ref. [9], except that the authors of that work investigated the comparison between charge integration and zero-crossing methods using analog PSD techniques.

3.3 PSD for different sized detectors

In addition, the two liquid scintillation detectors mentioned in Section 2.2 were tested using a ^{252}Cf source

Table 1. FOMs for different integration and differentiation time constants (C_1R_1, R_2C_2).

C_1R_1/ns	R_2C_2/ns	FOM	C_1R_1/ns	R_2C_2/ns	FOM
6	18	0.87	2	30	0.87
6	22	0.89	3	30	0.89
6	26	0.89	4	30	0.90
6	30	0.90	5	30	0.91
6	34	0.86	6	30	0.90
6	38	0.82	7	30	0.86
6	40	0.80	8	30	0.85

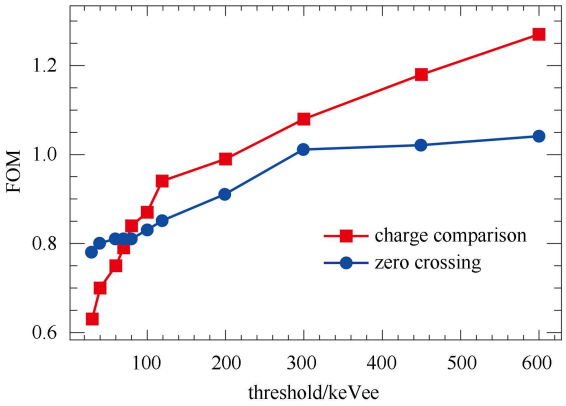

Fig. 7. (color online) Comparison of FOMs from charge integration and zero-crossing methods at different energy thresholds.

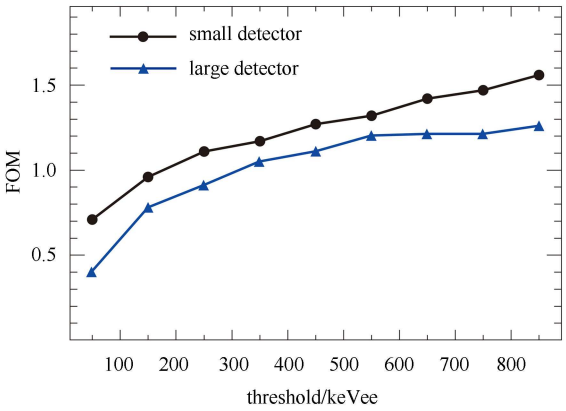

Fig. 8. (color online) Comparison of FOM for different size detectors at various energy thresholds.

to compare the capacity for n-γ discrimination of detectors of different sizes. The results calculated using the charge comparison algorithm are shown in Fig. 8. Significantly, the smaller liquid scintillation detector has greater FOM than the larger one at every energy threshold. This is perhaps because of the longer path of photon transportation in liquid scintillator for the larger one, which distorts the time information at the tails of pulses. Consequently, for fission neutrons, small dimension detectors are more universally used to minimize the distortion of neutron properties. If the experimental conditions are available, we plan to study the PSD properties of EJ-301 liquid scintillation detector through digital signal processing techniques for the ADS and SNS spallation targets in the future.

4 Summary

A digital acquisition system based on the NI-5772 adapter module for n-γ discrimination was established and tested with a ^{252}Cf neutron source. This system eliminates the need for QDC, TAC, delay cable etc. which are used in analog PSD techniques. The integration charge and zero-crossing time can be extracted through processing the digital waveforms off-line.

The energy calibration for the EJ-301 liquid scintillation detector was done using ^{22}Na, ^{137}Cs and ^{60}Co sources, and the γ response function was obtained as L=4.94E_e−0.095. Two different digital PSD algorithms were used to perform the n-γ discrimination of the EJ-301 liquid scintillation detector: the charge comparison method and the zero-crossing method. Both algorithms clearly showed the power of a digital system in achieving good PSD. The digital charge comparison method presented the optimum n-γ separation when the integration of slow components started 21 ns after the pulse maximum. At energy thresholds of 80 keVee and lower, the zero-crossing method gives better n-γ discrimination. At higher energies, the charge comparison method presents better separation between neutron and γ-ray events. In addition, for liquid scintillation detectors of different dimensions, a smaller detector showed better n-γ discrimination property for fission neutrons. In conclusion, the experimental results showed that such digital signal processing techniques could be very efficient for n-γ discrimination in mixed radiation fields.

The authors appreciate the support of the staff who maintain the LabVIEW software package. We would also like to thank Dr M. Nakhostin for his help in data processing.

References

1 Bowman C D, Arthur E D, Lisowski P W et al. Nucl. Instrum. Methods Phys. Res. A, 1992, **320**: 336–367
2 ZHAN W L, XU H S. Bulletin of Chinese Academy of Sciences, 2012, **03**: 375–381 (in Chinese)
3 Krivopustov M I, Chultem D, Adam J et al. Kerntechnik, 2003, **68**: 48
4 CHEN Y H, LEI J R, ZHANG X D et al. Chinese Physics C, 2013, **37**(4): 046202-1
5 Pai S et al. Nucl. Instrum. Methods A, 1989, **278**: 749
6 Kaschuck Y, Esposito B. Nucl. Instrum. Methods A, 2005, **551**: 420
7 Wolski D, Moszynski M, Ludziejewski T et al. Nucl. Instrum. Methods A, 1995, **360**: 584
8 M. Nakhostin, P. M. Walker. Nucl. Instrum. Methods A, 2010, **621**: 498–501
9 R. Aryaeinejad, Edward Reber, and Dave Spencer. IEEE Trans. Nucl. Sci, 2002, **49**(4): 1909–1913
10 Dietze G. IEEE Trans. Nucl. Sci, 1979, **NS-26**: 398–402
11 Dietze G, Klein H. Nucl. Instrum. Methods A, 1982, **193**: 549
12 ZHANG S Y L T, CHEN Z Q et al. Chinese Physics C, 2013, **37**(12): 126003
13 HUANG H X, RUAN X C et al. Chinese Physics C, 2009, **33**(8): 677–681